

Rhodocetin, a Novel Platelet Aggregation Inhibitor from the Venom of *Calloselasma rhodostoma* (Malayan Pit Viper): Synergistic and Noncovalent Interaction between Its Subunits^{†,‡}

Runhua Wang,[§] R. Manjunatha Kini,^{||} and Max C. M. Chung^{*,§,⊥}

Department of Biochemistry, Bioprocessing Technology Centre, and Bioscience Centre, National University of Singapore, Singapore, and Department of Biochemistry and Molecular Biophysics, Medical College of Virginia, Virginia Commonwealth University, Richmond, Virginia

Received September 2, 1998; Revised Manuscript Received January 28, 1999

ABSTRACT: A novel platelet aggregation inhibitor, rhodocetin, was purified from the crude venom of *Calloselasma rhodostoma*. It inhibited collagen-induced platelet aggregation in a dose-dependent manner, with an IC₅₀ of 41 nM. Rhodocetin has a heterodimeric structure with α and β subunits, which could be separated on a nonreducing denaturing gel or reverse-phase HPLC column. Individually neither subunit inhibited platelet aggregation even at 2.0 μ M concentration. Titration and reconstitution experiments showed that, when these subunits are mixed to give a 1:1 complex, most of its biological activity was recovered. The reconstituted complex inhibited platelet aggregation with an IC₅₀ of 112 nM, about 3-fold less effective than the native molecule. Circular dichroism analysis revealed that the reconstituted complex had a spectrum similar to that of the native protein. By using surface plasmon resonance studies, we established that the stoichiometry of binding between the two subunits is 1:1 and the subunits interact with a K_d of 0.14 ± 0.04 μ M. The complete amino acid sequences of the α (15956.16 Da, 133 residues) and β (15185.10 Da, 129 residues) subunits show a high degree of homology with each other (49%) and with the Ca²⁺-dependent lectin-related proteins (CLPs) (typically 29–48%) isolated from other snake venoms. Unlike the other members of the family in which the subunits are held together by an interchain disulfide bond, rhodocetin subunits are held together only through noncovalent interactions. The cysteinyl residues forming the intersubunit disulfide bridge in all other known CLPs are replaced by Ser-79 and Arg-75 in the α and β subunits of rhodocetin, respectively. These studies support the noncovalent and synergistic interactions between the two subunits of rhodocetin. This is the first reported CLP dimer with such a novel heterodimeric structure.

Snake venoms contain a variety of proteins that affect platelet aggregation and blood coagulation, important cellular and noncellular processes, respectively, in thrombosis and hemostasis (1). These proteins differ in their size and catalytic capabilities. There exists among them a group of nonenzymatic proteins that is structurally homologous to animal Ca²⁺-dependent lectins. These proteins show $M_r \sim 30000$ and exist as heterodimers linked by a single interchain disulfide bond. They share a structural homology between 30% and 70%. However, this group of Ca²⁺-dependent lectin-related proteins (CLPs)¹ exhibits different effects on blood coagulation and platelet aggregation. Some of these proteins exhibit anticoagulant activities by binding to the coagulant factors X and/or IX; for example, ECLV IX/X-bp from *Echis carinatus*

leucogaster venom (2); jararaca IX/X-bp from *Bothrops jararaca* venom (3), and habu IX/X-bp and IX-bp from *Trimeresurus flavoviridis* venom (4, 5). In contrast, bothrajaracin from *Bothrops jararaca* venom (6) is a specific inhibitor of thrombin. Several other CLPs induce varied effects on platelet functions by modulating the interactions between von Willebrand factor (vWF) and platelet glycoprotein Ib (GPIb). For example, botrocetin from *Bothrops jararaca* venom binds to vWF and forms an activated complex that induces platelet agglutination (7). On the other hand, alboaggregins from *Trimeresurus albolabris* venom (8, 9), echicetin from *Echis carinatus* venom (10), and agkicetin from *Agkistrodon acutus* venom (11) all bind to platelet GPIb and function as receptor blockers for vWF binding. However, alboaggregins induce platelet agglutination whereas echicetin and agkicetin inhibit platelet agglutination. Other platelet GPIb-binding proteins include flavocetin-A and -B from *Trimeresurus flavoviridis* venom (12), tokaracetin from *Trimeresurus tokarensis* venom (13),

[†] This work was supported by a NUS research scholarship to R. H. Wang.

[‡] The amino acid sequences of the α and β subunits have been deposited with the SWISS-PROT protein sequence database with the accession number P81397 and P81398, respectively.

^{*} To whom correspondence should be addressed. Phone: (65) 874 3252. Fax: (65) 7791453. E-mail: bchem@nus.edu.sg.

[§] Department of Biochemistry, National University of Singapore.

^{||} Bioscience Centre, National University of Singapore, and Virginia Commonwealth University.

[⊥] Bioprocessing Technology Centre, National University of Singapore.

¹ Abbreviations: CLPs, C-type lectin-related proteins; vWF, von Willebrand factor; PE, pyridylethyl; RP-HPLC, reverse-phase high-performance liquid chromatography; FPLC, fast protein liquid chromatography; SDS-PAGE, sodium dodecyl sulfate–polyacrylamide gel electrophoresis; CD, circular dichroism; BIA, biomolecular interaction analysis.

and jararaca GPIb-bp from *Bothrops jararaca* venom (14, 15). The structural basis for this diversity in functions is unknown. The question of whether the α - or β -subunit is responsible for the biological activity of CLPs has not been resolved (16). Thus, the elucidation of the structure–function relationships of this class of proteins is an interesting and challenging biochemical problem.

In the present study, we report the isolation and characterization of rhodocetin, a potent inhibitor of platelet aggregation from the venom of *Calloselasma rhodostoma* (Malayan pit viper). It has a heterodimeric structure, and individually both α and β subunits fail to show significant inhibition of aggregation. We have examined the synergistic and noncovalent interaction between these subunits. Amino acid sequence data indicates that rhodocetin is closely related to CLPs. This is the first CLP dimer which is held together by noncovalent interactions and not an interchain disulfide bond.

EXPERIMENTAL PROCEDURES

Materials. Crude venom of *Calloselasma rhodostoma* was purchased from Sigma Chemical Co. (St. Louis, MO). Collagen, thrombin, and ATP were products of Chronolog (Havertown, PA). Chymotrypsin was obtained from Boehringer Mannheim, while endoproteinase Lys-C was from Wako Pure Chemicals (Japan). FPLC and HPLC columns were from Amersham-Pharmacia and Vydac, respectively, and peptide sequencing chemicals/reagents were from PE-ABD (Foster City, CA). All buffer salts and organic solvents were from standard commercial sources and of the highest quality available.

Purification of Rhodocetin. *Calloselasma rhodostoma* crude venom (100 mg) was dissolved in 3.0 mL of 0.1 M ammonium hydrogen carbonate (pH 8.0) and centrifuged at 12000 rpm for 10 min at 4 °C to remove particulate material. (a) The supernatant was then fractionated by a HiLoad Superdex 75 column (2.6 \times 60 cm) equilibrated with the same buffer using a FPLC system. (b) The fractions from peak III (containing proteins of interest) were pooled and loaded directly onto a Mono Q HR 5/5 anion exchange column pre-equilibrated with 20 mM Tris-HCl, pH 8.2. (c) Fractions from peak 2 of Mono Q were buffer exchanged with 50 mM potassium phosphate, pH 7.0, containing 1.7 M ammonium sulfate (NAP-25 column) before being loaded onto a Phenyl-Superose HR 5/5 column equilibrated with the same buffer. Elution was performed at a flow rate of 0.5 mL/min with a linear gradient of 1.7–0.85 M ammonium sulfate in 50 mM potassium phosphate, pH 7.0, over 30 min.

Separation of Subunits. Subunits of purified rhodocetin were separated by reverse-phase HPLC using a pH stable C₈ Vydac column (4.6 \times 250 mm) on a Beckman System Gold Chromatograph. Solvents A and B were 0.1% (v/v) trifluoroacetic acid (TFA) and 0.085% (v/v) TFA in 70% (v/v) acetonitrile, respectively. Elution was performed using a linear gradient of 5–65% B in 45 min at a flow rate of 1 mL/min.

Molecular Weight Determination. Molecular weights of the native protein and its subunits were determined by gel filtration or electrospray mass spectrometry.

(A) **Gel Filtration.** The native molecular weight of rhodocetin was estimated by gel filtration chromatography on a Superose 12 HR 10/30 column using a FPLC system.

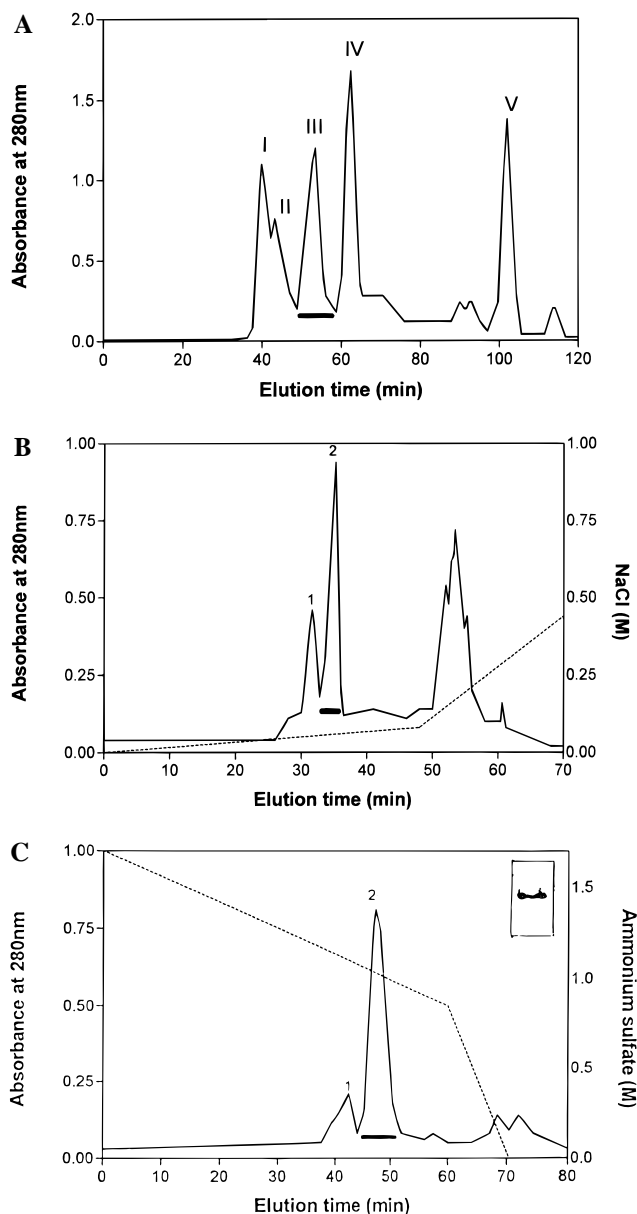


FIGURE 1: Purification of rhodocetin. (A) Gel filtration chromatography of *C. rhodostoma* crude venom on a HiLoad 26/60 Superdex 75 column. Elution was performed at 2 mL/min. (B) Anion exchange chromatography on a Mono Q HR 5/5 column. Proteins were eluted at 1 mL/min with a linear gradient of 0.00–0.08 M NaCl over 48 min. (C) Hydrophobic interaction chromatography on a Phenyl-Superose HR 5/5 column. (Inset) Nondenaturing PAGE of purified rhodocetin.

The column was equilibrated and eluted with 0.1 M ammonium hydrogen carbonate at a flow rate of 0.3 mL/min. Molecular marker proteins used included glutamate dehydrogenase (290 000), lactate dehydrogenase (142 000), enolase (67 000), adenylate kinase (32 000), and cytochrome C (12 400) (Oriental Yeast Company, Japan).

(B) **Electrospray Mass Spectrometry.** Mass spectrometry was carried out using a Perkin-Elmer Sciex API 300 LC/MS/MS system, a triple-stage quadrupole instrument equipped with an ionspray interface. The ionspray voltage was set to 4000 V, orifice voltage at 75 V, and the interface temperature at 60 °C. Nitrogen was used as a curtain gas with a flow rate of 0.6 L/min and as a nebulizer gas at 30 psi. Shimadzu LC-10AD series pumps were used for solvent delivery.

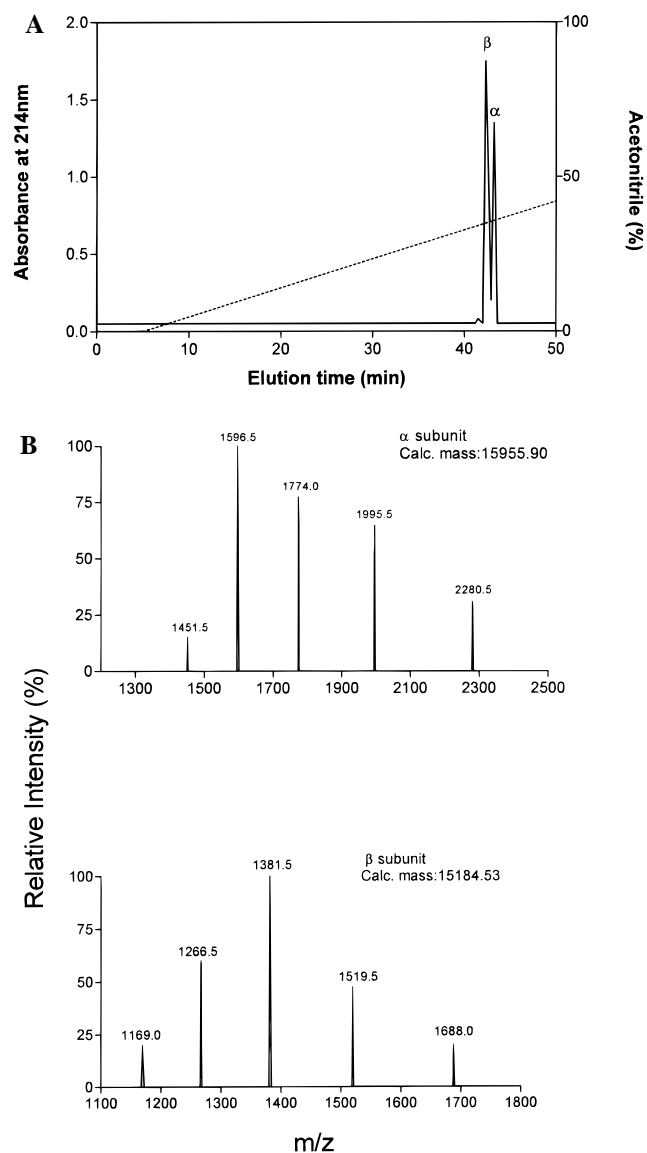


FIGURE 2: Separation of rhodocetin subunits. (A) Separation of the α and β subunits of rhodocetin by reverse-phase HPLC (RP-HPLC). The protein content was detected by absorbance at 214 nm. (B) Electrospray mass spectrometry spectra of rhodocetin subunits.

Polyacrylamide Gel Electrophoresis. Nonreducing and reducing (5% 2-mercaptoethanol) SDS-PAGE experiments were performed as described previously (17). Nondenaturing polyacrylamide gel electrophoresis was performed in the absence of SDS.

Determination of the Isoelectric Point. The isoelectric point of rhodocetin was determined using agarose IEF at a pH range of 3–10 (Pharmalyte) on the basis of the manufacturer's protocol.

Enzymatic Digestion. The α and β subunits were first reduced and *s*-pyridylethylated (*s*-PE) on the basis of the method of Polgar et al. (16). Proteolytic digestions were performed in 100 mM Tris-HCl, pH 9.2 (endoproteinase Lys C), and 100 mM sodium hydrogen carbonate, pH 7.8 (α -chymotrypsin), at an enzyme/substrate ratio of 1:50. Denaturation and solubilization of substrates were enhanced by the inclusion of 6 M urea and incubation at 37 °C for 1 h. Prior to the addition of enzymes, the concentration of urea

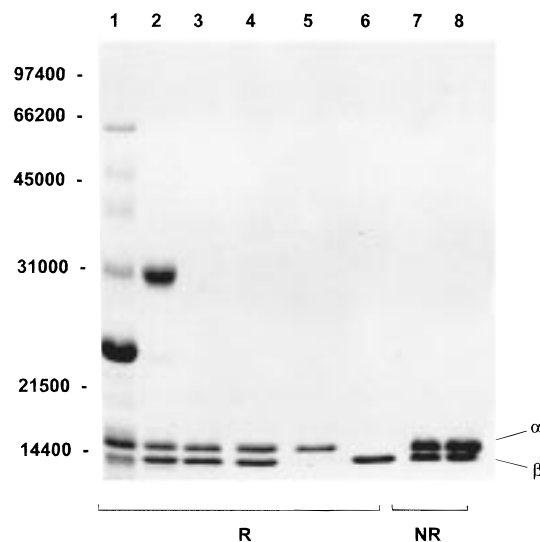


FIGURE 3: SDS-PAGE analysis of rhodocetin and its subunits under nonreducing (NR) and reducing (R) conditions. SDS-PAGE was performed using 12.5% separating gel: lane 1, crude venom of *C. rhodostoma*; lane 2, peak III from gel filtration; lanes 3 and 7, peak 2 from anion exchange chromatography; lanes 4 and 8, peak 2 (rhodocetin) after HIC; lane 5, α subunit; and lane 6, β subunit from HPLC. Molecular masses of the markers are indicated on the left.

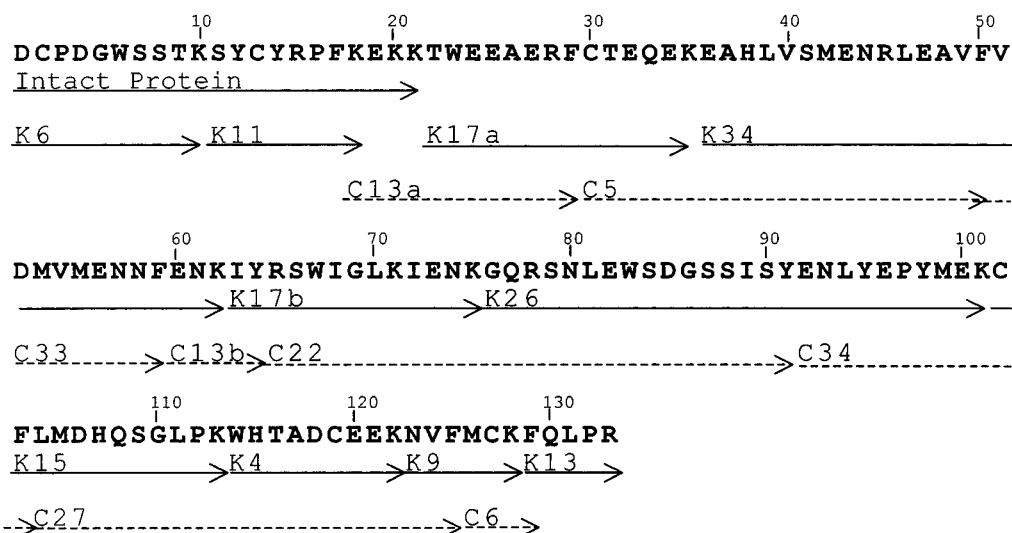
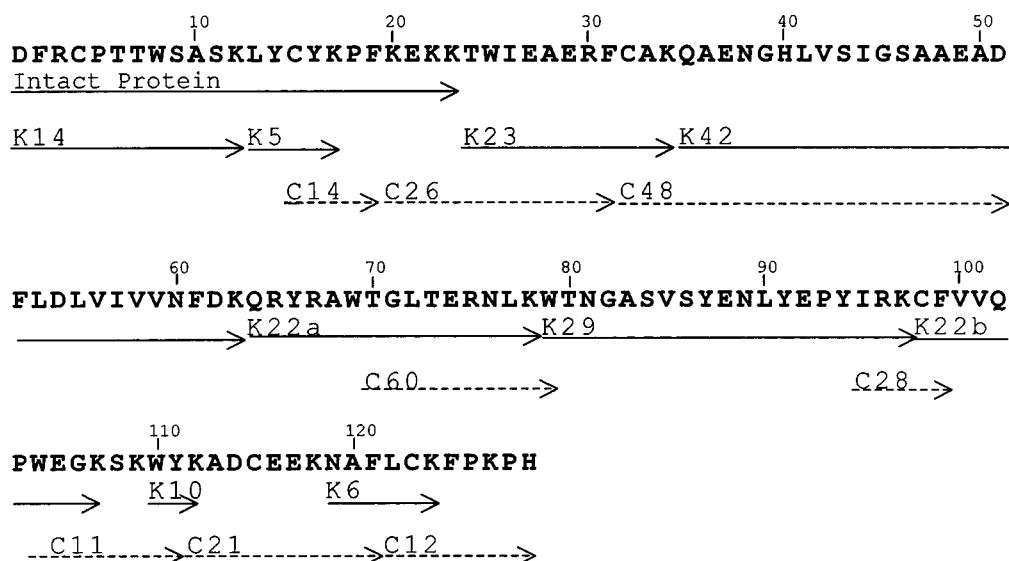
was reduced to 2 M, and subsequent incubation was performed at 37 °C overnight. Each digest was fractionated by a μ RPC C₂/C₈ column (2.1 \times 100 mm, 3 μ m particle size, with a pore diameter of 120 Å) using a linear gradient of 0.05% TFA/water (v/v) and 0.05% TFA/100% acetonitrile (v/v) in a Pharmacia SMART system. Detection was at 214 nm.

Peptide Sequencing. The N-terminal amino acid sequences of the subunits of rhodocetin and their internal peptides were determined by automated Edman degradation using an Applied Biosystems 477A pulsed liquid-phased sequencer equipped with an on-line PTH amino acid analyzer (120A). The masses of selected peptides were also determined by electrospray ionization (ESI) mass spectrometry as described above.

Renaturation and Reconstitution of Rhodocetin Subunits. The α and β subunits of rhodocetin from reverse-phase HPLC were concentrated by Speedvac and renatured by gel filtration chromatography (Superose 12 HR 10/30 column) (18) in 100 mM ammonium hydrogen carbonate, pH 7.8. These renatured fractions of the α and β subunits were then reconstituted at different molar ratios and allowed to incubate overnight at 4 °C.

Circular Dichroism Studies. CD studies were carried out with a Jasco J-715 spectropolarimeter. The cuvette chamber of the spectropolarimeter was continuously purged with pure nitrogen before and during the experiment. Measurements were made in 20 mM Tris-HCl, pH 8.2. The spectra were measured between 260 and 200 nm in a 1 mm path length cell at room temperature, using a 2.0 nm bandwidth, a 0.1 nm step, and a 4 s time constant. The results were expressed as the molar ellipticities (θ).

Biomolecular Interaction Analysis (BIA). The interactions of the α and β subunits of rhodocetin were monitored by surface plasmon resonance (SPR) using a BIAcore2000 instrument (Pharmacia Biosensor). Briefly, a CM5-sensor

A Rhodocetin- α Rhodocetin- β 

B

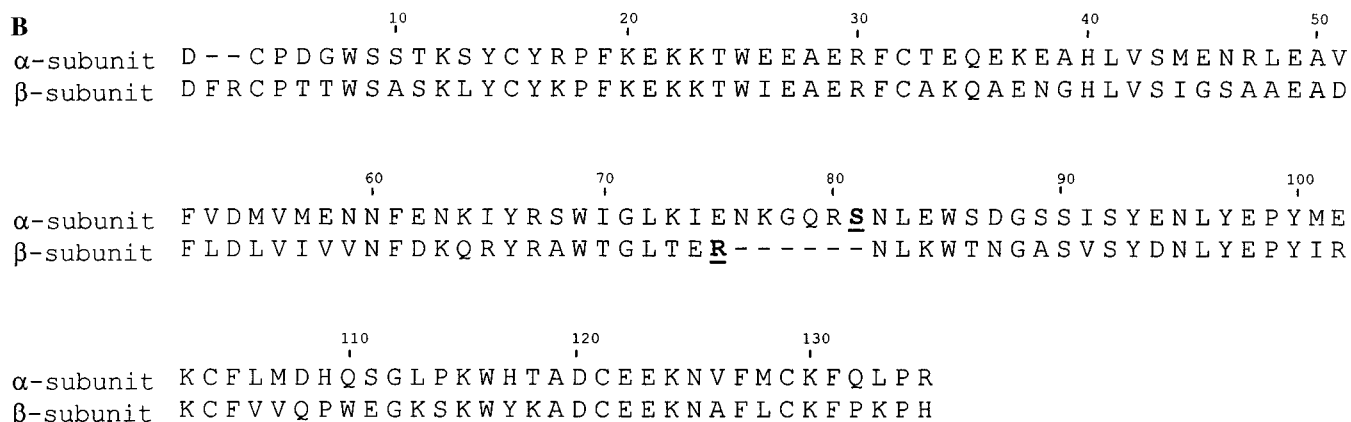


FIGURE 4: Complete amino acid sequences of the α and β subunits of rhodocetin. (A) Determination of the complete sequences of the α and β subunits. The prefixes K and C denote peptides generated by cleavage of the PE- α and PE- β subunits of rhodocetin with endoproteinase Lys-C and α -chymotrypsin, respectively. (B) Sequence comparison of the α and β subunits. The 2 amino acid residues that always form the single intersubunit disulfide bond between them are *underlined*.

chip was preactivated with an amine coupling kit for 6 min at a flow rate of 5 μ L/min, followed by blocking of unac-

tivated sites with 1 M ethanolamine for 2 min. Approximately 600 resonance units (RU) of renatured rhodocetin α subunit

was then immobilized by passing 100 $\mu\text{g/mL}$ of α subunit diluted in a coupling buffer, pH 7.0, over the preactivated sensor chip for 2 min at a flow rate of 5 $\mu\text{L/min}$. Renatured β subunit diluted to final concentrations of 25–250 $\mu\text{g/mL}$ in HEPES-buffered saline (HBS) was then passed over the coated sensor chip at a flow rate of 5 $\mu\text{L/min}$ for 10 min. Dissociation was then observed by passing HBS sample buffer over the sensor chip. Association and dissociation rate constants were calculated using the BIA Evaluation program 3.0, assuming the relationship $A + B = AB$.

Coagulation Assays. The effect of venom proteins on blood coagulation was determined by prothrombin time (19). Male rabbits weighing 3–4 kg were bled from the central artery of the ear. Human blood was drawn from healthy volunteers who were not taking any medication. Blood was anticoagulated with 0.11 M trisodium citrate (1: 9, v/v). Plasma was obtained by centrifugation of the blood for 10 min at 4000g. Venom proteins (50 μL of 0.5 mg/mL in 0.15 M Tris-HCl buffer, pH 7.4) were preincubated for 2 min at 37 °C with 100 μL of rabbit plasma and 50 μL of 0.15 M Tris-HCl buffer, pH 7.4. Clot formation was initiated by the addition of 200 μL of thromboplastin with calcium (Sigma Chemical Co.) to the mixture, and coagulation times were measured in a BBL fibrometer.

Platelet Aggregation. Whole blood aggregation was measured by the impedance method described by Cardinal and Flower (20), using a whole-blood aggregometer (Chronolog, Havertown, PA). Anticoagulated rabbit and human blood, collected as described above, was diluted with phosphate-buffered saline (PBS) (1:1). Diluted blood (1 mL) was prewarmed with various concentrations of protein solution (50 μL) for 2 min at 37 °C. Platelet aggregation was initiated by the addition of platelet agonists (collagen, 2 $\mu\text{g/mL}$; thrombin, 0.2 IU/mL; ADP, 10 μM). All aggregation tests were performed in quadruplicate. The percent inhibition was calculated by comparing the impedance of the aggregation curves 5 min after the addition of platelet agonists, taking the impedance of the control curve as 100% aggregation.

RESULTS

Purification of Rhodocetin. The crude venom of *Calloselasma rhodostoma* was separated into five main fractions by gel filtration chromatography (Figure 1A). The SDS electrophoretic patterns of these fractions are shown in Figure 3. Fraction III, which displayed potent inhibitory activity on collagen-induced platelet aggregation, was thus selected for further fractionation by anion exchange chromatography (Figure 1B) and hydrophobic interaction chromatography (Figure 1C). Peak 2 (Figure 1C), which exhibited a single band on a nondenaturing gel (Figure 1C, insert) and two bands in SDS-PAGE either in the presence or absence of reducing agent (DTT or 2-mercaptoethanol) (Figure 3), was designated as rhodocetin. The isoelectric point of purified rhodocetin was determined to be 8.15 (results not shown).

Separation of Rhodocetin Subunits. When subjected to RP-HPLC, purified rhodocetin was separated into two subunits (Figure 2A). The first and second peaks, which had molecular masses of 15 and 16 kDa, were designated as β and α subunits, respectively (see also Figure 3).

Molecular Weight Determination. The native molecular weight of rhodocetin was determined to be 35 000 by gel

Table 1: Mass Spectrometric Analysis of α and β Subunits and Purified Peptides from Endoproteinase Lys-C Digestion of Rhodocetin

peptides	residue no.	calculated ^a	observed ^b
α Subunit			
intact	1–133	15956.16	15955.90 \pm 1.44
K4	114–122	1222.18	1222.61 \pm 0.17
K6	1–10	1199.44	1199.71 \pm 0.42
K9	123–128	847.34	847.50 \pm 0.20
K11	11–18	1167.50	1167.86 \pm 0.49
K13	129–133	659.78	660.50 \pm 0.13
K15	102–113	1479.65	1480.49 \pm 0.61
K17a	22–35	1890.90	1891.65 \pm 0.47
K17b	63–71	1135.66	1136.16 \pm 0.34
K26	76–101	3082.37	3082.55 \pm 0.42
K34	36–62	3195.49	3196.09 \pm 0.43
β Subunit			
intact	1–129	15185.10	15184.53 \pm 2.74
K5	13–17	794.50	794.50 \pm 0.71
K6	119–124	799.84	799.77 \pm 0.23
K14	1–12	1503.53	1503.77 \pm 0.38
K22a	64–78	1891.30	1891.53 \pm 0.15
K22b	98–107	1297.36	1297.04 \pm 0.42
K23	24–34	1458.53	1458.27 \pm 0.26
K29	79–97	2290.46	2290.46 \pm 0.48
K42	35–63	3071.80	3073.19 \pm 0.65

^a Molecular masses calculated from the amino acid sequences of the denoted peptides. ^b Molecular masses calculated from multiple charged signals observed.

filtration (data not shown). However, in both reducing and nonreducing SDS-PAGE, rhodocetin showed two bands with M_r values of 16 000 (α subunit) and 15 000 (β subunit) (Figure 3). After RP-HPLC, the α and β subunits, when analyzed by electrospray mass spectrometry, yielded molecular masses of 15955.90 \pm 1.44 and 15184.53 \pm 2.74 Da, respectively (Figure 2B). Furthermore, native rhodocetin also showed two molecular masses of 15954.96 \pm 0.82 and 15185.35 \pm 1.41 Da, which were in agreement with the individual molecular masses for the α and β subunits, respectively.

Amino Acid Sequence of Rhodocetin. The complete amino acid sequences of both of the subunits of rhodocetin were determined by sequencing individual subunits and the peptides generated by the reduced and *s*-pyridylethylated subunits. The sequences of the overlapping peptides and other details of the sequencing strategy are summarized in Figure 4A. The amino acid sequence data was corroborated with mass spectrometric data. The calculated molecular masses of the endoproteinase Lys-C (K-peptides), the α (133 amino acid residues, 15 956.16 Da), and the β subunits (129 amino acid residues, 15 185.10 Da) were in agreement with their respective masses observed by mass spectrometric analyses (Table 1). Moreover, the α and β subunits of rhodocetin also show a high degree of homology between them (49% identity) (Figure 4B).

Sequence Comparison of Rhodocetin with CLPs from Other Snake Venom. When aligned with those of other known members of the CLP superfamily from snake venoms (Figure 5), the α and β subunits of rhodocetin showed 42–56% and 29–48% sequence identity to the α and β subunits of botrocetin (21), alboaagreggin-B (22), echicetin (16, 23), ECLV IX/X-bp (2), Habu IX/X-bp (4), and habu IX-bp (5), respectively.

All of the intramolecular half-cysteinyl residues in the sequences of α and β subunits of rhodocetin and other CLPs

α subunits

Rhodocetin	D--CPDGWSSSTKSYCYRPFKEKKTWEEAEERFCTEQEKEAHLVSMEN--RLAEVFDVMMENNENFKTIYRS--WIGLKIEKNGQQRNLEWSDGSSISYENLY
AL-B	D--CPSDWSSFKQYCYQIFKQLKTWEDAEERFCMDQVKGALVSIYESYR--EAVFVAQQLSENKTKY--DWIGLSVNVKGGQSSSEWSDGSSSVSYENLV
Bothrajaracin	D--CPSDWSSHEGHCYKFFQKMNWADAERFCSEQAAGGHLVSFQS--DGETDFVNLVTEKIQSTD--YAWIGLRVQNKKEQCSSKWSGSSSVSYENNV
Botrocetin	D--CPSGWSSYEGNCYKFFQKMNWADAERFCSEQAAGGHLVSIKISKEKDFVGLDVTNKTQSSDL--YAWIGLRVENKEKQCSSEWSDGSSSVSYENNV
Echicetin	DQDCLSGWSSFYEGHCYQLERLLKTWDEAEKYC--NQWDGGHLVSIES--NAKAEFVAQLISRLPKSAIEDRWVWIGLRDRSKREQGGHLWTNDSFVHYEHVV
ECLV IX/X-bp	D--CLPGWSSHEGHCYKVENYKTKWDAEKFCCKGKSGHLVSVES--SEEGDFVAKLISENLEKSHSIDFVWTGLTYKGRWKQCSSEWSDGSKIKYQKWG
Habu IX/X-bp	D--CLSGWSSYEGHCYKAFKFKYKTIWEDAEERFCTEQAKGHLVSIES--SGEADFVAQLVTQNMKRLDF--YIWI GLRVQKVKQCNSEWSDGSSSVSYENWI
Habu IX-bp	D--CLSGWSSYEGHCYKPFKLYKTWDDAEERFCTEQAKGHLVSIES--AGEADFVAQLVTENIQNTKS--VWIGLRVQKKEKQCSSEWSDGSSSVSYENWI
Jararaca GPIb-bp	D--CPSDWSPYGGHCYKLFKQRMNWAENLCAQQRKESHLVSFHS--SEEVDLVLSTFPILGPDLY---WTGLS--NIWNGCSFEQSDGTKNVYNANA

Rhodocetin	EPYMEKCFMLDHQSGLPKWHITADCEEKNVFMCKQLPR
AL-B	KPLSKKCFVLKKGTEFRKWNVACEQKHLFVCKFLRPR
Bothrajaracin	GRIVKKCFALEKEQEFFWVINIYCGQGNPFVCK--SPPP
Botrocetin	ERTVKKCFALEKDLGFVLWINLYCAQKNPFVCK--SPPP
Echicetin	PP--TKCFVLERQTEFRKWIANCFEKFPPFVCKAFIPR
ECLV IX/X-bp	KQOPRKCLGLEKQTEFRKWVNLCEEPQRTCEI
Habu IX/X-bp	EAESKTCLEKETDFRKWNLYCGQGNPFVCE--A
Habu IX-bp	EAESKTCLEKETGFRKWVNLCEEPQRTCEI
Jararaca GPIb-bp	SE--SECVA-SKITD-NQWSPFCIRLQYFVCEFA

 β subunits

Rhodocetin	DFRCPTIWSASKLYCYKPFKEKKTWEEAEERFCAQQAENGHLVSISSAAEADFLDLVIVNFDKQRYRAWTGLTER---NLKWTNGASVSYENLYEPIYIR
AL-B	D--CPSDWSSYDLYCYRVFQEKKNWEDAEKFCCTQHTDHLVSFDSSEEDFVASKTFFVLKHLV--WIGLGSVNVACKLQWSDGTGLKYNA---WSA
Bothrajaracin	D--CPPDWSSYEGSCYRVFEQKMNWEDAEKFCCTQQTGGHLVSFQSSEEDFVSLTSPILRDSFV--WTGLSDVWKECFEWSGSDLSYKINYQVFS
Botrocetin	D--CPPDWSSYEGHCYRFFKEKMWDDAEERFCTEQQTGAHLVSFQSKEEDFVRSLSLSEMLKGDVV--WIGLSDVWVKCFEWDQMEFDY--DDY--YLIA
Echicetin	N--CLPDWSSYEGCYKVFKEKMNWEDAEKFCCTQHTDHLVSFDSSEEDFVSLTSPILRDSFV--WIGLSDVWVKCFEWDQMEFDY--DDY--YLIA
ECLV IX/X-bp	D--CSSGWTAYGKHCYKVFDEPKTIWEDAEKFCSEQAAGGHLVSFRSSKEADFVVTLTATQTESEIV--WMGLSKITWQCNQWGWINGAKINYE--WAEA
Habu IX/X-bp	D--CPSDWSSYEGHCYKPFSEPKNWAENFCTQHGAGHLVSFQSSEEDFVVKLARQTFGHSIF--WMGLSNVNVQCNQWWSNAMLRYKA---WAE-

Rhodocetin	KCFVVOQFWEKSKWYKADCEEKNFLCKFFKPH
AL-B	ESECITSKSTINEWLTRCSRTPYFVCKFQ--A
Bothrajaracin	EYECVASKTKNNKWRILPCTKLEYFVCEFQ--A
Botrocetin	EYECVASKPTNNKWWILPCTRFKNFVCEFQ--A
Echicetin	ERHCFAAKTITNQMRRKCSGEFYFVCKCP--A
ECLV IX/X-bp	ESYCVWFSSSTNKWKSRPCSLFGHFVCKSP--A
Habu IX/X-bp	ESYCVYFKSTNNKWRSRACRMMAQFVCEFQ--A

FIGURE 5: Sequence comparison of rhodocetin with related CLPs. The α and β subunits of rhodocetin are aligned with those of botrocetin (19), alboaggregin-B (20), echicetin (16, 21), ECLV IX/X-bp (2), habu IX/X-bp (4), and IX-bp (5), respectively. Numbers indicate positions of amino acid residues from the amino termini of the α and β subunits of rhodocetin. Gaps (—) have been introduced to maximize homology.

are also conserved, but rhodocetin is devoid of a half-cysteinyl residue at positions 79 and 75 in the α and β subunits, respectively (Figure 4). These corresponded to residues number 84 and 79, respectively, in Figure 5, due to the gaps being used to align the sequences. These two residues have been found to form the only intersubunit disulfide bond in all of the other known CLPs. The lack of cysteinyl residues forming the interchain disulfide bond explains the ease of separation of subunits in rhodocetin.

Reconstitution of Rhodocetin Complex. Reconstitution of the rhodocetin complex was achieved by simply combining the two subunits in 100 mM ammonium hydrogen carbonate, pH 7.8, and incubating overnight at 4 °C. Gel filtration chromatography on a Superose 12 column showed that the retention time/volume of the reconstituted complex was similar to that of native rhodocetin (data not shown). The interaction between α and β subunits and the formation of rhodocetin complex at a molar ratio of 1:1 was further supported by BIA and CD analyses as well as functional assays of platelet aggregation (see below).

To examine the stoichiometry and the affinity between the subunits, we examined the rhodocetin complex formation using BIA analysis. The binding sensorgrams for the interaction of the various amounts of β subunit (25–250 μ g/mL)

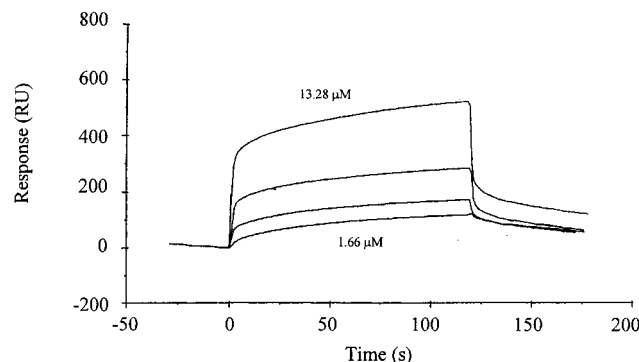


FIGURE 6: Binding curves of β subunit to the α subunit coated sensor chips. The binding sensorgrams were obtained by passing different concentrations of renatured β subunit over the sensor chip that had been immobilized with renatured α subunit.

with immobilized α subunit were presented in Figure 6. It showed that the binding between the α and β subunits of rhodocetin had a stoichiometry of 1:1. The association and dissociation constants, as calculated for binding of β to α subunits over a range of four different concentrations, were $(1.27 \pm 0.36) \times 10^5 \text{ M}^{-1} \text{ s}^{-1}$ and $(1.71 \pm 0.32) \times 10^{-2} \text{ M}^{-1} \text{ s}^{-1}$, respectively. A K_D value of $0.14 \pm 0.04 \mu\text{M}$ was thus

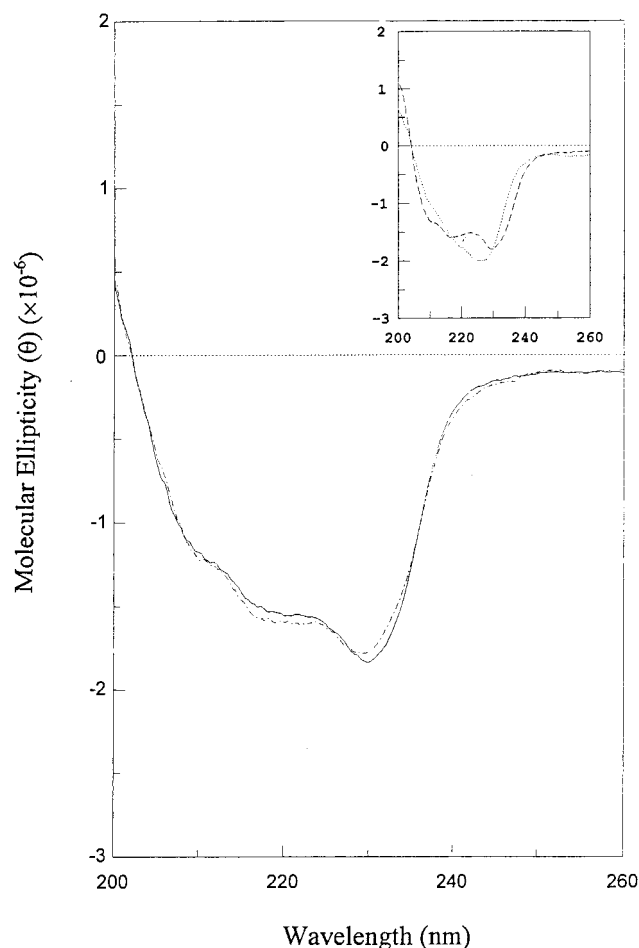


FIGURE 7: CD spectra of native rhodocetin and its reconstituted 1:1 complex. CD spectra were measured by using a 1 mm path length cell as described in the Experimental Procedures. The concentrations of native rhodocetin, its subunits, and reconstituted complex were 3.1–4.4 μM . (Inset) The CD spectra of individual α and β subunits. Native rhodocetin (—); reconstituted complex (---); α subunit (---); β subunit (···).

calculated from the ratio of dissociation and association rate constants.

CD analysis showed that there was no significant conformational change between native rhodocetin and its reconstituted α and β subunits (Figure 7). However, the CD spectra for the individual α and β subunits exhibit some differences (Figure 7, inset).

Effect of Rhodocetin and Its Reconstituted Complex on Blood Coagulation and Platelet Aggregation. Rhodocetin and its reconstituted 1:1 complex had no effect on blood coagulation as determined by the prothrombin times of rabbit and human plasma. However, rhodocetin showed a potent inhibitory effect on platelet aggregation in rabbit whole blood induced by collagen (2 $\mu\text{g}/\text{mL}$) (Figure 8A), but not by ADP (10 μM) or thrombin (0.2 IU/mL) (Figure 8C). Similar results were obtained using human whole blood (Figure 8D). For rabbit whole blood, the inhibition was dose-dependent with an IC_{50} of 1.3 $\mu\text{g}/\text{mL}$ (41 nM) (Figure 8A,B). Individually neither α nor β subunit exhibited any significant inhibitory effect even at a concentration of 2.0 μM (Figure 8B). This indicates that both subunits are essential for the inhibition of platelet aggregation. Upon reconstitution and formation of the 1:1 complex, the inhibition of platelet aggregation was regained. The reconstituted complex exhibited dose-depend-

ent inhibition of aggregation with an IC_{50} of 3.6 $\mu\text{g}/\text{mL}$ (112 nM). Thus about a third of the inhibitory property was regained upon reconstitution.

The synergistic interaction between the α and β subunits of rhodocetin and the role of synergism in the inhibitory effect of platelet aggregation in rabbit blood could be elegantly demonstrated by a titration experiment (Figure 8E). In this experiment, the concentration of α subunit was kept constant at 100 nM, while different concentrations of β subunit were added. As expected, increasing amounts of β subunit induced higher inhibition of platelet aggregation. The percentage of inhibition reached the optimum plateau when the concentration of β subunit was about 100 nM. The addition of higher amounts of β subunit did not significantly enhance the inhibition. Thus maximal effects were achieved only at a stoichiometry of 1:1. These results further support the complex formation and synergism between the two subunits.

DISCUSSION

Ca^{2+} -dependent lectin-related proteins (CLPs) isolated from snake venoms are a structurally homologous group of proteins. They are heterodimers comprising of α and β subunits with M_r values of about 14–15000. Each subunit has seven half-cysteiny residues forming three intrachain disulfide bridges, and the seventh cysteine forms an inter-chain disulfide bond linking the two subunits. The subunits bear a high degree of sequence homology with each other and with the other snake venom CLPs. Despite their striking structural similarity, this group of proteins has a variety of biological effects (see Introduction). In addition, some of these proteins are lectins and they exhibit mitogenic activity (24, 25). Thus structure–function relationships of this group of proteins are complicated and interesting.

We report here the purification and characterization of a unique CLP dimer, rhodocetin, from the venom of *Calloselasma rhodostoma*. In marked contrast to all the known proteins from this superfamily, the two subunits of rhodocetin are not linked by any intersubunit disulfide bonds. In rhodocetin, the α subunit consists of 133 amino acids residues (M_r , 15 956), while the β subunit, 129 amino acid residues (M_r , 15 185). However, the α and β subunits of rhodocetin contain only six half-cysteiny residues each. The positions of six half-cysteiny residues are conserved, and they are present at the same locations as those of the intrachain cysteine residues, for example, botrocetin (Figure 9) and the other CLPs (Figure 5). From the known disulfide pairings of CLPs, we could infer that the intrasubunit disulfide bonds of rhodocetin may occur as follows: α subunit, 2–13, 30–127, and 102–119; and β subunit, 4–15, 32–123, and 98–115 (Figure 9). However, as expected, rhodocetin is devoid of a half-cysteiny residue each at position 79 of the α subunit and at position 75 of the β subunit (Figure 4A). Since these two half-cysteiny residues always form the only intersubunit disulfide bridge that is found in all other CLPs, rhodocetin is thus a snake venom CLP with a unique structure in which the subunits are held together only by noncovalent interaction. By using surface plasmon resonance (SPR) studies, we further corroborated the interaction between the subunits; we were able to demonstrate unequivocally that the stoichiometry between the renatured α and β subunits was 1:1 and the K_D for this

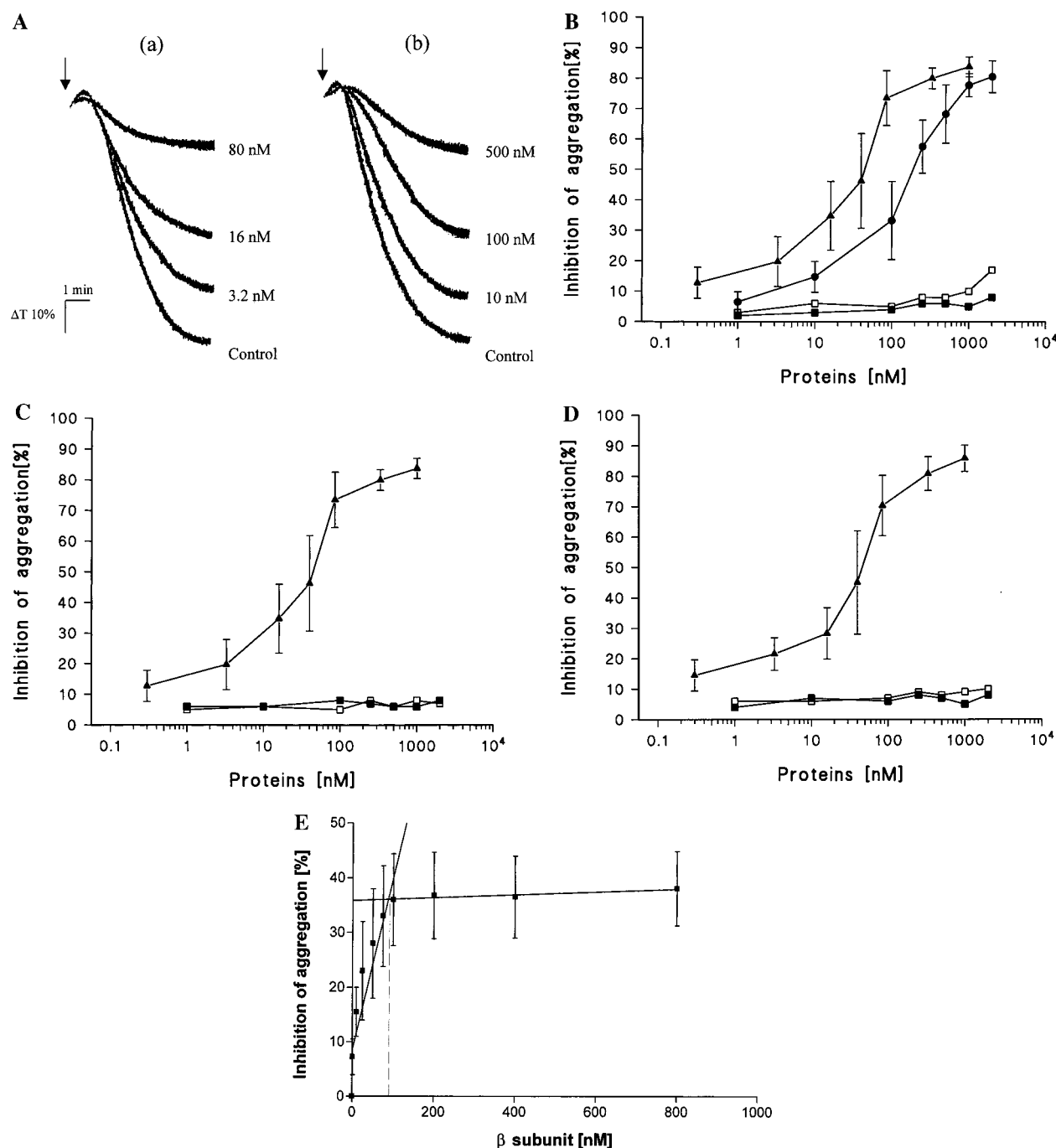


FIGURE 8: Inhibition of collagen-induced platelet aggregation by rhodocetin, individual α and β subunits, and reconstituted 1:1 complex. (A) Tracings of the inhibitory effects of rhodocetin and its reconstituted complex on platelet aggregation in rabbit whole blood: (a) rhodocetin; and (b) reconstituted α and β subunits. (B) Percentage of inhibition of platelet aggregation in rabbit whole blood by rhodocetin, individual α and β subunits, and reconstituted complex: (●) reconstituted complex; (▲) rhodocetin; (■) α subunit; (□) β subunit. (C) Inhibitory effects of rhodocetin on platelet aggregation in rabbit whole blood induced by various agonists: (▲) collagen (2 $\mu\text{g}/\text{mL}$); (■) ADP (10 μM); (□) thrombin (0.2 IU/mL). (D) Inhibitory effects of rhodocetin on platelet aggregation in human whole blood induced by various agonists: (▲) collagen (2 $\mu\text{g}/\text{mL}$); (■) ADP (10 μM); (□) thrombin (0.2 IU/mL). (E) Titration of rhodocetin β subunit with α subunit in platelet aggregation in rabbit whole blood. Values are presented as means \pm SE ($n = 4$).

interaction is 0.14 μM . Several specific protein–protein interactions in nature, for example, the one between coagulation factors X_a and V_a , are in the same range (26). Conformational analysis using CD indicates that the overall conformation of the reconstituted 1:1 complex of rhodocetin is similar to that of the native molecule (Figure 7). We have also demonstrated the importance of this interaction to the biological activity of rhodocetin (Figure 8). Thus rhodocetin is a first example of a CLP dimer in which both subunits

act synergistically to exhibit the biological activity, and these subunits are held together by noncovalent interactions.

Two of the hurdles in understanding the structure–function relationships of snake venom CLPs are to recognize whether one or both subunits are required for biological activity and to identify which subunit plays an important role in the activity. Rhodocetin is a potent inhibitor of platelet aggregation induced by collagen. The subunits can be separated easily by reverse-phase HPLC. As shown here, both subunits

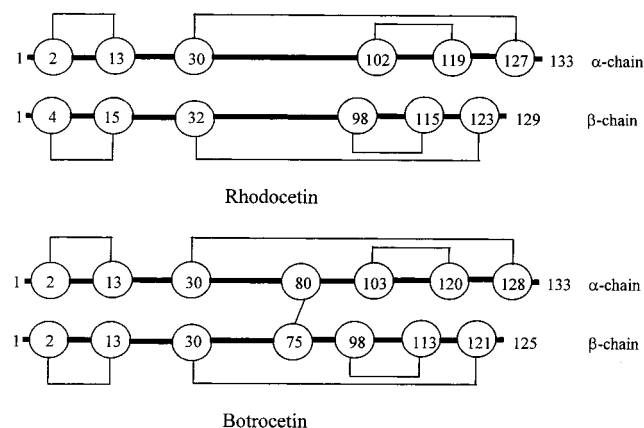


FIGURE 9: Comparison of the locations of the disulfide bridges between rhodocetin and botrocetin. Bold lines indicate peptide chains; fine lines indicate disulfide bridges; numbers indicate positions of amino acid residues from the amino termini of α and β subunits; and circled numbers indicate positions of half-cysteinyl residues.

are essential for the inhibition of platelet aggregation. Neither α subunit nor β subunit significantly inhibits the platelet aggregation (Figure 8B). The reconstituted complex inhibits collagen-induced aggregation. We have also demonstrated that the formation of 1:1 complex is important for the biological activity of rhodocetin. In contrast, some of the earlier studies have shown that the biological activity was attributable to its β subunit. Peng et al. showed that the reduced and alkylated β subunit of echicetin retained inhibitory activity (23). In the case of *jararaca* GPIIb-IIIb the reduced but not alkylated β subunit retained its biological activity (15). However, Polgar et al. reported that neither reduced and alkylated α and β subunits of echicetin inhibited the platelet agglutination (16). One of the difficulties with these previous studies is the requirement for the CLPs to be completely denatured, reduced, and carboxymethylated before the subunits could be isolated for subsequent binding experiments. Thus although the β subunit is important for the biological effects in the above cases, it is not clear whether the loss of activity for the α subunit is due to a change in the conformation. Unlike the other CLPs, the two subunits of rhodocetin act synergistically for the expression of its biological activity. The second subunit helps to have a close to native conformation and biological activity.

Recently, Shin and Morita (27) reported the isolation and characterization of rhodocytin, a novel platelet agonist from the same snake venom. Rhodocytin has a dimeric disulfide-linked structure, which is characteristic of the known CLPs. In fact, we have also isolated and partially characterized a protein with similar structural and functional properties to rhodocytin in the course of this work (28). This CLP, present in peak I (Figure 1A), was further purified by anion exchange chromatography (Mono Q) at pH 8.2 (28). The dimer, under reducing conditions in SDS-PAGE, gave two bands with molecular masses of 18.7 (α) and 14.7 (β) kDa, respectively. The N-terminal amino acid sequences of the α and β subunits and the effects of this protein on platelets are also identical to those of rhodocytin (27, 28). However, this protein probably has a quaternary structure consisting of at least two disulfide-linked dimers since it has a native molecular weight of about 66 000 as determined by gel filtration (28). This structural information was not evident from the work on

rhodocytin (27) and the earlier publication of Huang et al. on aggrexin (29). It is interesting to note that the venom of *Calloselasma rhodostoma* is the source of three novel toxins, as exemplified by the two novel CLPs reported here, as well as a major hemorrhagin (rhodostoxin) that contained the first four disulfide-linked proteinases reported among all known venom metalloproteinases (30).

In conclusion, we have purified and characterized a novel CLP in which the two subunits are held together only by noncovalent interaction and not by any interchain disulfide bridge. Both subunits are essential for the potent inhibition of platelet aggregation. Further studies are underway to examine the mechanism of inhibition of platelet aggregation and structure-function relationships of rhodocetin.

ACKNOWLEDGMENT

We wish to thank Dr. Tan Yee Joo from the Institute of Molecular and Cell Biology (IMCB), National University of Singapore, for assistance with BIA analysis.

REFERENCES

- Kornalik, F. (1991) In *Snake Toxin* (Harvey, A. L., Ed.) pp 323–383, Pergamon Press, New York.
- Chan, Y. L., and Tsai, I. H. (1996) *Biochemistry* 35, 5264–5271.
- Sekiya, F., Atoda, H., and Morita, T. (1993) *Biochemistry* 32, 6892–6897.
- Atoda, H., Hyuga, M., and Morita, T. (1991) *J. Biol. Chem.* 266, 14903–14911.
- Atoda, H., Ishikawa, M., Yoshihara, E., Sekiya, F., and Morita, T. (1995) *J. Biochem.* 118, 965–973.
- Zingali, R. B., Jandrot-Perrus, M., Guillin, M. C., and Bon, C. (1993) *Biochemistry* 32, 10794–10802.
- Fujimura, Y., Titani, K., Usami, Y., Suzuki, M., Oyama, R., Matsui, T., Fukui, H., Sugimoto, M., and Ruggeri, Z. M. (1991) *Biochemistry* 30, 1957–1964.
- Peng, M., Lu, W., and Kirby, E. P. (1991) *Biochemistry* 30, 11529–11536.
- Peng, M., Lu, W., and Kirby, E. P. (1992) *Thromb. Haemostasis* 67, 702–707.
- Peng, M., Lu, W., Bevilacqua, L., Niewiarowski, S., and Kirby, E. P. (1993) *Blood* 81, 2321–2328.
- Cheng, Y. L., and Tsai, I. H. (1995) *Biochem. Biophys. Res. Commun.* 210, 472–477.
- Taniuchi, Y., Kawasaki, T., Fujimura, Y., Suzuki, M., Titani, K., Sakai, K., Kaku, S., Hisamichi, N., Satoh, V., Takenaka, T., Handa, M., and Sawai, Y. (1995) *Biochim. Biophys. Acta* 1244, 331–338.
- Kawasaki, T., Taniuchi, Y., Hisamichi, N., Fujimura, Y., Suzuki, M., Titani, K., Kaku, S., Satoh, N., Takenaka, T., Handa, M., and Sawai, Y. (1995) *Biochem. J.* 308, 947–953.
- Fujimura, Y., Ikeda, Y., Miura, S., Yoshida, E., Shima, H., Nishima, S., Suzuki, M., Titani, K., Taniuchi, Y., and Kawasaki, K. (1995) *Thromb. Haemostasis* 74, 743–750.
- Kawasaki, T., Fujimura, Y., Usami, Y., Suzuki, M., Miura, S., Sakurai, Y., Makita, K., Taniuchi, Y., Hirano, K., and Titani, K. (1996) *J. Biol. Chem.* 271, 10635–10639.
- Polgar, J., Magnenat, E. M., Peitsch, M. C., Wells, T. N. C., Saqi, M. S. A., and Clementson, K. J. (1997) *Biochem. J.* 323, 533–537.
- Laemmli, U. K. (1970) *Nature* 227, 680–685.
- Werner, M. H., Clore, G. M., Gronenborn, A. M., Kondoh, A., and Fisher, R. J. (1994) *FEBS Lett.* 345, 125–130.
- Quick, A. J. (1966) In *Haemorrhagic Diseases and Thrombosis* (Quick, A. J., and Febiger, L., Eds.) 2nd ed., pp 391–395, Philadelphia, PA.
- Cardinal, D. C., and Flower, R. J. (1982) *J. Pharmacol. Methods* 3, 135–158.

21. Usami, Y., Fujimura, Y., Suzuki, M., Ozeki, Y., Nishio, K., Fukui, H., and Titani, K. (1993) *Proc. Natl. Acad. Sci. U.S.A.* 90, 928–932.
22. Usami, Y., Suzuki, M., Yoshida, E., Sakurai, Y., Hirano, K., Kawasaki, T., Fujimura, Y., and Titani, K. (1996) *Biochem. Biophys. Res. Commun.* 219, 727–733.
23. Peng, M., Holt, J. C., and Niewiarowski, S. (1994) *Biochem. Biophys. Res. Commun.* 205, 68–72.
24. Ozeki, Y., Matsui, T., Hamako, J., Suzuki, M., Fujimura, Y., Yoshida, E., Nishida, S., and Titani, K. (1994) *Arch. Biochem. Biophys.* 308, 306–310.
25. Mastro, A. M., Hurley, D. J., Winning, R. K., Filipowski, R., Ogilvie, M. L., and Gartner, T. K. (1986) *Cell Tissue Kinet.* 19, 557–566.
26. Boskovic, D. S., Giles, A. R., and Nesheim, M. E. (1990) *J. Biol. Chem.* 265, 10497–10505.
27. Yongchol, S., and Morita, T. (1998) *Biochem. Biophys. Res. Commun.* 245, 741–745.
28. Thiang, K. S. C., and Chung, M. C. M. (1998) in *Proceedings of the Fourth National Undergraduate Research Opportunities Programme (NUROP)*, Vol. 1, pp 29–32, National University of Singapore, Singapore.
29. Huang, T.-F., Liu, C.-Z., and Yang, S.-H (1995) *Biochem. J.* 309, 1021–1027.
30. Chung, M. C. M., Ponnudurai, G., Kataoka, M., Shimizu, S., and Tan, N. H. (1996) *Arch. Biochem. Biophys.* 325, 199–208.

BI982132Z